Guidelines for Pelvis and Spine Positioning of Human Body Models for Application in Occupant Protection Simulations.

Yash Kumar Vari, Giacomo Marini, Kilian Wagner[1]

Abstract

In recent years, human body models (HBMs) have become widely popular in vehicle safety analyses, and with the forthcoming virtual testing, it is relevant to define harmonised initial posture definition for virtual testing applications. Current Euro NCAP positioning protocol provide a standardised approach to defining global hip joint centre (HJC) and seat locations, but they do not provide a method for defining pelvis and spine orientation across HBMs. This study proposes a cross-model procedure for defining nominal pelvis and upper-spine posture in adult male 50th percentile (AM50) HBMs in occupant protection simulations. First, pelvis and lumbar spine geometries from five AM50 HBMs (THUMS, GHBMC, ViVA+, SAFER and HANS) were compared in a common local HJC-centred coordinate system, and pelvis-angle definitions were evaluated using sagittal-plane root-mean-square (RMS) dispersion of anterior superior iliac spine (ASIS) and pubic symphysis landmarks. Second, individual-level reclined passenger-posture data were reanalysed using linear mixed-effects models (LMMs) to predict pelvis angle and HJC-centred locations of key spinal joints namely thoracolumbar junction (T12-L1), cervicothoracic junction (C7-T1), and atlanto-occipital joint (C0-C1). Third, the resulting LMM-predicted nominal posture values were implemented in a marionette-method positioning workflow and applied to the three complete AM50 HBMs available in Virtual Performance Solution Pam-Crash for final implementation in this study (THUMS, GHBMC, and ViVA+). The HJC-ASIS pelvis angle definition produced the lowest combined ASIS + pubic symphysis RMS dispersion, 6.77 mm, compared with 9.14 mm for the next-best evaluated definition, sacral slope. The LMMs predicted pelvis angle with a root-mean-square error (RMSE) of approximately 11° and spinal joint coordinates with RMSE values ranging from 17 to 34 mm. The results indicate that the proposed procedure provides a practical workflow for harmonised initial HBM positioning in occupant protection simulations.

Keywords Euro NCAP, Human body model, Pelvis orientation, Spine posture, Upright seating.

I. INTRODUCTION

Several Human Body Models (HBMs) are currently being used alongside Anthropomorphic Test Devices (ATDs) for investigating occupant injury and to support consumer assessment activities [1–3]. HBMs provide a more detailed description of the anatomy and posture as compared to ATDs, and they enable the evaluation of internal loads, organ responses and detailed kinematics in different loading and seating conditions [1]. Each HBM is based on different anthropometric data and modelling approaches [4–9]. These anthropometric and modelling differences result in geometric differences between HBMs even when they are representing the same percentile, for example, the adult male 50th percentile (AM50) models. These differences complicate direct comparison across HBMs and may allow model choice to influence the interpretation of simulation outcomes [4–7].

The European New Car Assessment Programme (Euro NCAP) has introduced protocols for the qualification and use of HBMs in frontal impact simulations (CP-550 Qualification Procedure for HBMs v1.1 and CP-551 HBM Simulation for Frontal Impacts v1.1) [2-3]. The CP-551 v1.1 protocol defines target seat position and target hip joint centre (HJC) locations based on seat configurations and anthropometric variables [3]. However, the spinal orientation is advised to be kept fixed, and there is no range or definition given for the pelvis orientation [3]. Different users can position similar percentile HBMs with different pelvis angles or upper-body alignment, which could affect belt path, torso orientation, and crash kinematics [10-11].

The pelvis orientation is of special interest, as the interaction of the lap-belt with the bony pelvis, particularly the anterior superior iliac spine (ASIS) and anterior region of iliac crest, has a significant impact on the submarining phenomenon and abdominal loading, which has been demonstrated in various experimental, imaging, and

[1]Y. K. Vari is a MSc student in Mechanical Engineering at Otto Von Guericke University in Magdeburg. G. Marini is a safety engineer at Audi AG, Ingolstadt, Germany (giacomo.marini@audi.de, +4915257719789), K. Wagner is a safety engineer at Audi AG.

computational studies [11–14]. Additionally, reclined seating has been shown to have a significant impact on the pelvis orientation, particularly in rotating the pelvis backwards in a posterior direction with increasing seatback angle [15–17]. The spinal curvature and the alignment of head-torso have also been found to have a significant impact on the global kinematics and load paths in frontal impact crashes [10][16][18]. Several pelvis angle and spinal posture definitions have been proposed in the literature (e.g. Nyquist pelvic angle, sacral slope, segment-based spinal angle definitions) [14–16][19]. However, no harmonised cross-HBM procedure is currently provided for defining pelvis and spine orientation of AM50 HBMs in virtual-testing workflows.

In literature several studies are available, which investigated occupant posture by measuring specific anatomical reference points. Reed, Ebert and colleagues have characterised reclined seating posture and belt fit using segment-based spinal angles and pelvis orientation [15][17]. Izumiyama have examined skeletal alignment and its effect on seatbelt kinematics using HBMs and imaging data [16]. Tanaka have analysed lap-belt fit to human subjects using CT imaging, and Forman et al. have explored variability in soft-tissue geometry and belt fit [14][20]. In the present study, the Reed and Ebert 2018 study dataset was selected as the primary statistical source because it provides individual-level automotive passenger-posture data across multiple seatback angles and headrest conditions, together with anthropometric variables and skeletal joint centre estimates derived from digitized surface landmarks [15]. Comparable individual-level datasets from other published studies were considered, but were not available to the authors at the time of analysis or used a different type of seat (rigid seat) or used a different approach for defining the pelvis and spinal orientation which was challenging to be integrated for harmonised HBM pelvis and spine positioning [14][16][20].

The objective of the study is to develop an anatomy-based cross-model procedure for pelvis and spine positioning that is aligned with the Euro NCAP HBM positioning procedure and can support harmonised HBM positioning in occupant protection simulations [3].

II. METHODS

The methodology was organized into three stages. First, a cross-model pelvis-angle comparison was performed using pelvis and lumbar geometries from five AM50 HBMs namely THUMS, GHBMC, ViVA+, SAFER, and HANS [4–7][21]. This stage evaluated which sagittal pelvis-angle definition provided the lowest root-mean-square (RMS) dispersion of the ASIS and pubic symphysis landmarks after HJC-based translation and sagittal rotation. These two landmarks were used because they could be consistently identified across all five pelvis geometries. Second, individual-level volunteer posture data from the reclined passenger-seat study (Reed and Ebert 2018) were reanalysed to derive linear mixed-effects models (LMMs) [15]. These LMMs were used to predict nominal pelvis and upper-spine posture values in an HJC-centred sagittal coordinate system. Third, the resulting LMM-predicted nominal posture values were implemented in three complete AM50 HBMs (THUMS, GHBMC and ViVA+) available in the study environment Virtual Performance Solution Pam-Crash (VPS) using a marionette-method based positioning workflow [4–6][22]. SAFER and HANS were included only in the pelvis-angle comparison because the isolated pelvis and lumbar-spine finite-element (FE) mesh geometries were available, but complete models suitable for the final marionette-method based implementation were not available in VPS [7][21]. This workflow was used to develop a candidate cross-model procedure for harmonised initial pelvis and upper-spine positioning in occupant protection simulations.

Cross Model Pelvis Comparison Study

The purpose of the cross-model pelvis-angle comparison was to evaluate which sagittal pelvis-angle definition best aligned the consistently identifiable anterior pelvis landmarks namely ASIS, pubic symphysis after HJC-based translation across the five available AM50 HBM pelvis geometries. The pelvis and lumbar spine geometry of five AM50 HBMs (THUMS v7.1, GHBMC v4.5, ViVA+ v2.0.1, SAFER v11.2.0 and the HANS v1.4) were included in the pelvis comparison study [4–7][21]. An overview of the five AM50 HBMs considered in the study is provided in Appendix Fig. A1.1. Soft-tissue margins were not included in the cross-model pelvis comparison study because the purpose was limited to comparing skeletal-anterior pelvis landmark alignment across pelvis geometries. Therefore, effects of abdominal and thigh soft tissue were outside the scope of this geometric comparison.

The analysis was performed in the sagittal X-Z plane. The X-axis was defined positive posteriorly, the Y-axis laterally, and the Z-axis superiorly. The sagittal plane refers to the X-Z plane through the midline of the pelvis. The vertical reference was the positive Z direction, and the horizontal reference was the X direction. The coordinate system used for the pelvis comparison was aligned with the seat-based global reference system used later for HBM positioning. Fig. 1 shows the coordinate axes and anatomical landmarks used in the study.

In each HBM, the surface nodes of the acetabulum were chosen, and a sphere was fitted to these nodes by the least squares method, as described in the Euro NCAP CP-551 protocol [3]. The script provided in the Open VT portal for the calculation of the HJC was used to calculate the HJC of each pelvis geometry [3]. The centre of the fitted sphere was used as the HJC. The fitted sphere radius was recorded as a diagnostic value because it reflects the local acetabulum geometry and the quality/sensitivity of the sphere fit. The fitted radii were subsequently compared across models as part of the evaluation of HJC estimation sensitivity.

The midpoint between the left and right HJCs was then calculated and projected to the sagittal plane by setting the lateral coordinate to zero. This projected midpoint is referred to as the mid-HJC and was used as the local HJC origin for the sagittal pelvis-angle comparison. Unless otherwise stated, HJC-centred sagittal coordinates in this study refer to coordinates expressed relative to this projected mid-HJC.

Thereafter, the following pelvis-angle definitions were evaluated:

- **HJC-L5-S1 angle (HJLS):** angle between the mid-HJC and the lumbosacral joint (L5-S1) centre relative to the vertical in sagittal plane [15]. For interpreting this definition consistently with different HBMs, the centre of gravity (COG) of the L5-S1 was considered.
- **Nyquist pelvic angle (NPA):** angle between the pubic symphysis (pubic crest) and ASIS relative to the vertical in sagittal plane [14][19]. Nyquist originally defined the pelvis angle using the pubic symphysis and ASIS line relative to the global horizontal. In this work, the same anatomical landmarks were retained, but the angle was defined relative to the global vertical so that one consistent reference system could be used throughout the study and aligned with later literature using the vertical reference [14][19].
- **Sacral slope (SS):** angle of the superior endplate of the S1 vertebrae relative to the horizontal in sagittal plane [16].
- **ASIS-L5-S1 angle (ASLS):** angle between the ASIS point and L5-S1 joint centre relative to the vertical in the sagittal plane.
- **HJC-ASIS angle (HJAS):** angle between the mid-HJC and the ASIS relative to the vertical in sagittal plane.

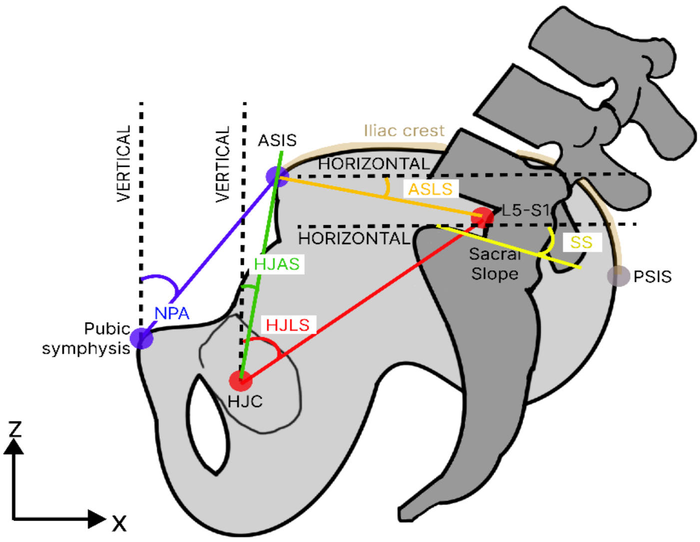

Fig. 1. Pelvis angle definitions evaluated in the sagittal X-Z plane [14–16][19]. The X-axis is positive posteriorly and the Z-axis is positive superiorly; the Y-axis is lateral and is therefore not shown.

The pelvis landmarks were defined on the off-the-shelf HBM's geometry for the upright seating condition. The ASIS landmark was defined as the midpoint of the left and right most anterior ASIS nodes projected into the sagittal plane. The pubic symphysis landmark was defined as the average of the left and right most anterior pubic symphysis nodes projected into the sagittal plane. The L5-S1 joint centre was defined using the COG of the intervertebral disc when available. If explicit L5-S1 disc elements were not available, the local geometry near the base of the sacrum and lower surface of L5 vertebrae was used to approximate the COG as the joint centre. The angle between the ASIS and the posterior superior iliac spine (PSIS) relative to the horizontal called the ASIS-PSIS inclination [23], was not considered because of difficulties in consistently defining the PSIS landmark amongst the available HBM pelvis geometries.

Each pelvis geometry was initially translated so that its mid-HJC was located at the local sagittal coordinate origin (X = 0, Z = 0). After this translation, the mid-HJCs of all pelvis geometries coincided at the same origin. This step removed global position differences and allowed the pelvis-angle definitions to be compared using the same local HJC reference. No yaw or roll rotations were applied at this stage. In this configuration, substantial differences in alignment were observed in the ASIS and iliac crest region across HBMs, as well as differences in spinal curvature as shown in Fig. 2.

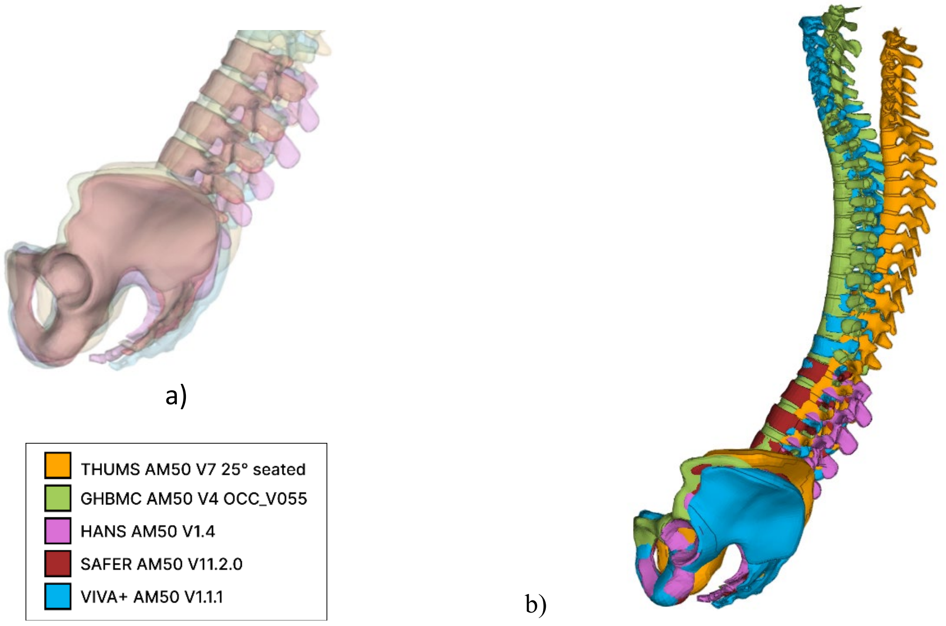

Fig. 2. Initial comparison of five HBM pelvis geometries after translation to a common local mid-HJC origin, without yaw or roll rotations. The complete spinal geometry of SAFER and HANS were not available

Later, each pelvis-angle definition was evaluated separately. For a given pelvis-angle definition, each pelvis geometry was rotated about the mid-HJC in the sagittal plane until that specific pelvis angle reached the value prescribed for comparison (e.g., 12° for HJAS pelvis angle definition). Because the initial pelvis orientations differed between models, the amount of rotation required was not necessarily the same for all pelvis geometries. This procedure was not used to impose a physiological posture, but to normalise the geometries so that same pelvis-angle definition could be compared across models.

Cross-model pelvis alignment was quantified using sagittal-plane RMS dispersion of the ASIS and pubic symphysis landmarks. These two landmarks were selected because they could be consistently identified and defined across all five HBMs. For each landmark and pelvis-angle definition, the centroid of the five HBM landmark coordinates was calculated. The Euclidean distance of each model-specific landmark the five-model centroid was then computed, and the RMS dispersion was calculated as

$$D_{\mathrm{RMS}} = \sqrt{\frac{1}{N}\sum_{i=1}^{N}\left[(x_i - \bar{x})^2 + (z_i - \bar{z})^2\right]} \quad (1)$$

where x_i and z_i are the sagittal-plane coordinates of the landmark for model i, and $\bar{x}$ and $\bar{z}$ are the corresponding five-model centroid coordinates, and N is the number of HBMs included in the comparison. Lower RMS dispersion indicates better cross-model alignment of the evaluated landmark. A combined anterior landmark score was calculated by pooling the ASIS and pubic symphysis landmark distances. Additionally, model-specific residual distances from the ASIS and pubic symphysis landmark centroids were also calculated to identify the deviation from the five-model landmark centroid.

The ASIS and pubic symphysis were used as the quantitative anterior pelvis landmarks because they could be consistently identified across all five evaluated HBM pelvis geometries. The iliac crest was not used as a quantitative landmark because it is a continuous curved anatomical ridge, and equivalent homologous points on the crest could not be defined with sufficient confidence across the different mesh topologies. The PSIS was also not used because it could not be identified consistently across all pelvis geometries. The iliac crest region was retained only as supporting visual/anatomical context and was not used to rank the pelvis-angle definitions.

Volunteer Posture Dataset and HJC-Centred Posture Variables

Statistical LMM-predicted nominal posture values were derived from the reclined passenger posture study of Reed and Ebert 2018 [15]. In that study, 24 adult volunteers (12 men, 12 women) with a wide range of stature, age and body mass index (BMI) were measured in a modified vehicle mock-up equipped with a six-way power front seat from a 2010 Toyota Highlander and a three-point belt system [15]. The seat pan angle was fixed at 14.5°, and the seat-back (SAE A40) was set to nominal angles of 23°, 33°, 43° and 53° using a power recliner [15]. Two headrest conditions were included, with headrest and without headrest. For each recline angle, postures were recorded with and without a participant-adjusted foam-padded head rest that provided comfortable static support, along with anthropometric variables: stature, erect sitting height (ESH), weight, BMI, age, gender [15].

Posture in the Reed and Ebert study was characterised using digitized body landmarks and estimated skeletal joint centres. Landmark locations on the participant, mock-up, seat, and belt were recorded using a FARO Arm coordinate digitizer. Because ASIS identification can be difficult in participants with higher adiposity, Reed and Ebert used a dedicated ASIS-location tool based on the participant's measured bi-ASIS breadth to assist palpation and digitization in the vehicle mock-up. Additional hard-seat measurements were used to access posterior spine and pelvis landmarks that were not easily accessible in the vehicle seat. The source study then estimated pelvis position, pelvis orientation, L5-S1, and HJCs using surface landmarks, flesh-margin corrections, and optimization procedures rather than direct skeletal imaging [15]. This introduces uncertainty when transferring the volunteer-derived posture variables to HBM landmark definitions.

This dataset was selected as the primary statistical source because it provided individual-level automotive passenger-posture data across multiple seatback angles and headrest conditions, together with the anatomical landmark information needed to construct HJC-centred pelvis and upper-spine posture variables. These characteristics made it more directly compatible with the present HBM-positioning workflow than datasets that report only group-level posture summaries, use different seat types like rigid seats, or used a different method for defining the pelvis and spine orientation [14][16][20]. Additionally, this dataset was the only available individual-level automotive passenger-posture dataset accessible to the authors that included the required landmark and anthropometric variables for constructing the HJC-centred pelvis and upper-spine posture representation.

An analysis-ready posture dataset was constructed from the individual-level data. The mid-HJC was calculated as the average of the left and right HJCs [15]. The ASIS midpoint was calculated as the average of the left and right bony ASIS landmarks. The pelvis angle was then calculated in the sagittal X-Z plane as the angle between the vertical direction and the vector from the mid-HJC to the ASIS midpoint [15].

The upper-spine posture was described using three anatomical levels in the study namely the thoracolumbar junction (T12-L1), the cervicothoracic junction (C7-T1), and the atlanto-occipital joint (C0-C1) [15]. The locations of these anatomical landmarks were expressed relative to the mid-HJC in the sagittal plane as shown in Fig. 3.

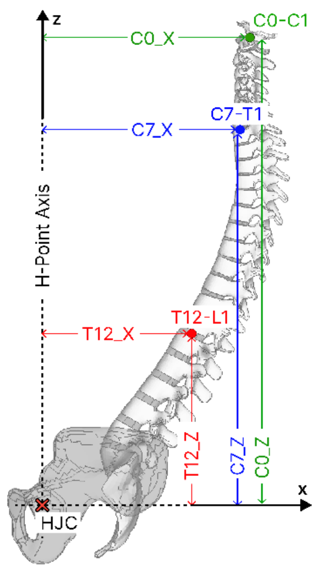

Fig. 3. HJC-centred cartesian representation of the pelvis and spine in the sagittal plane to define T12-L1, C7-T1, and C0-C1 coordinates.

T12_X and T12_Z represented the anterior-posterior and vertical coordinates of the T12-L1 joint centre relative to the mid-HJC, C7_X and C7_Z represented the corresponding coordinates of the C7-T1 joint centre, and C0_X and C0_Z represented the coordinates of the head-neck junction relative to the mid-HJC. The same sagittal coordinate convention defined initially in the cross-model pelvis comparison study was used for these HJC-centred variables. This HJC-centred coordinate system provided a consistent anatomical reference for describing upper-body posture across participants and provides a stable local anatomical origin for transferring posture information to HBMs. Expressing T12-L1, C7-T1, and C0-C1 relative to the mid-HJC also avoids propagating variability through intermediate spinal-segment definitions [15].

Statistical Modelling of Nominal Pelvis and Spine Posture

LMMs were used to derive the predicted nominal pelvis and upper-spine posture values [24]. LMMs were selected because the Reed and Ebert dataset contains repeated posture measurements from the same volunteers across multiple seatback angles and headrest conditions (up to eight combinations of multiple seat-back angle and headrest use for each volunteer). A simple independent-observation regression would not account for this within-subject dependence. In contrast, LMMs allow the population-average posture trend to be estimated while also accounting for subject-specific baseline posture differences and subject-specific responses to seatback recline [24].

Candidate predictors were seatback angle, headrest condition, age, BMI, ESH, standing stature without shoes, and gender. Headrest was coded as 0 = without headrest and 1 = with headrest. Gender was coded as 0 = female and 1 = male, following the coding of the source dataset. Seatback angle and headrest condition were treated as design/configuration variables and were retained in all models.

Before fitting the LMMs, multicollinearity among continuous anthropometric predictors was assessed using a correlation matrix and variance inflation factors (VIFs). The screened continuous anthropometric predictors were age, BMI, ESH, and standing stature without shoes. Stature and ESH were strongly correlated, so stature was removed and ESH was retained because it is more directly related to seated upper-body geometry. The final candidate predictor set for the LMMs was therefore seatback angle, headrest condition, age, BMI, ESH, and gender.

Separate LMMs were fitted for each of the seven outcomes namely Pelvis_Angle, T12_X, T12_Z, C7_X, C7_Z, C0_X, and C0_Z. The study did not fit a separate model for every subject-condition combination. Instead, one mixed model was fitted per outcome, and the repeated-measures structure was handled through random effects. For subject i in condition j, the full model had the form

$$\begin{aligned} Y_{ij} = \beta_0 + \beta_1 SeatbackAngle_{ij} + \beta_2 Headrest_{ij} + \beta_3 Age_i + \beta_4 BMI_i + \beta_5 ESH_i + \beta_6 Gender_i + u_{0i} \\ + u_{1i} SeatbackAngle_{ij} + \varepsilon_{ij} \end{aligned} \tag{2}$$

where Y_{ij} is the observed outcome value for subject i in condition j. β_0-β_6 are fixed effects, u_{0i} is the subject-specific random intercept, u_{1i} is the subject-specific random slope for seat-back angle, and ε_{ij} is the residual error term. Anthropometric variables (age, BMI, ESH, gender) were included only as fixed effects because they do not vary within subjects. Random slopes were only used for seat-back angle, which does vary within subjects. Seatback angle was included as a random slope because it varies within subjects and because different volunteers may respond differently to recline. Headrest was retained as a fixed effect. All LMMs were fitted using maximum likelihood (ML), rather than restricted maximum likelihood (REML), because the full and reduced models differed in their fixed-effect structure and were compared using likelihood-based information criteria [24].

For each outcome, a full LMM was first fitted with seatback angle, headrest, age, BMI, ESH, and gender as fixed effects, together with a subject-specific random intercept and a subject-specific random slope for seatback angle as defined in Equation 2. Thereafter, a reduced model was developed to retain the predictors that made a statistically significant and practically meaningful contribution, while keeping the model simple. Seatback angle and headrest were always retained as predictors because they define the seating condition. Age, BMI, ESH, and gender were retained as predictors only if they satisfied a predefined predictor selection criterion i.e., statistical significance ($p <= 0.05$) and a minimum effect over the observed predictor range. The effect over the observed range was defined as

$$\Delta Y_p = \beta_p \left(x_{max,p} - x_{min,p} \right) \tag{3}$$

where, ΔY_p is the predicted change in the outcome associated with predictor p across its observed range, β_p is the regression coefficient of predictor p and $x_{max,p}$ and $x_{min,p}$ are the maximum and minimum observed values of that predictor in the dataset, respectively. Equation (3) quantifies how much the predicted spinal joint position or pelvis angle changes when a predictor varies from its smallest to its largest observed value. Predictors were retained only if $\left|\Delta Y_p\right| \geq 5$ mm for spinal joint coordinates and $\left|\Delta Y_p\right| \geq 3°$ for pelvis angle. For gender, the effect reduced to the LMM coefficient itself.

After applying the predictor-selection rule, a reduced LMM was fitted for each outcome using seatback angle, headrest, and the retained anthropometric and gender predictor. Full and reduced LMMs were compared using Akaike information criterion (AIC). Bayesian information criterion (BIC) was additionally calculated as a supplementary check because it penalizes model complexity more strongly. AIC was used as the primary selection criterion. For each outcome, the difference was calculated as

$$\Delta AIC = AIC_{reduced\ model} - AIC_{full\ model} \tag{4}$$

$$\Delta BIC = BIC_{reduced\ \mathrm{model}} - BIC_{full\ \mathrm{model}} \tag{5}$$

The reduced model was retained when it had equal or lower AIC than the full model $(\Delta\mathrm{AIC} \leq 0)$ [25].

The final nominal posture values used for HBM positioning were obtained from the fixed-effect component of the final reduced LMMs. The random effects were used during model fitting to account for repeated measurements and subject-specific deviations, but they were not used to define the final nominal HBM posture. Therefore, the final positioning workflow used population-average fixed-effect predictions, rather than subject-specific predictions or averaged subject-level coefficients.

For a selected seatback angle, headrest condition, and anthropometric input set, the fixed-effect component of the final LMMs provides predicted nominal posture values for Pelvis_Angle, T12_X, T12_Z, C7_X, C7_Z, C0_X, and C0_Z. RMSE and MAE were calculated relative to the fixed-effects-only predictions. The residual for each observation was defined as

$$\mathrm{residual} = \mathrm{observed\ posture\ value} - \mathrm{population\ average\ fixed\ effect\ prediction} \tag{6}$$

Therefore, RMSE and MAE describe how much the actual observed volunteer postures from the Reed dataset deviate from nominal population-average posture. They were not calculated from coefficient averaging. Residual normality was assessed for each final reduced LMM outcome using the Shapiro-Wilk test [26]. The RMSE values were used to define practical engineering tolerance bands around the LMM-predicted nominal posture values. The ±1×RMSE band was considered a tighter practical positioning tolerance, and the ±2×RMSE band was considered a broader variability envelope. These tolerance bands were not treated as formal confidence intervals, and no exact 68% or 95% theoretical coverage was assumed.

To generate nominal posture values for THUMS AM50 Version 4.1, GHBMC M50 Version 4.5, and ViVA+ 50M seated Version 2.0.1, the LMMs were evaluated using one common set of AM50 anthropometric inputs. The selected values were male gender, age 39 years, BMI 24.9 kg/m², ESH 893.5 mm, seatback angle 23°, and no headrest, for this demonstration case. This was done to keep the statistical prediction of nominal posture values consistent across the three HBMs. Model-specific values were not used because equivalent published anthropometric data were not available for all models, especially for ESH. ESH depends on posture and therefore, estimating ESH separately from the default posture of each HBM would have been problematic, because the value would change again once the pelvis and spine were repositioned. For this reason, a single nominal input set was used for all three HBMs. These inputs were used only to generate the LMM-predicted nominal posture values for the application and should not be interpreted as a general AM50 population definition.

To transfer these LMM-predicted spinal posture values to HBMs, harmonised HBM landmark definitions were introduced for consistently identifying T12-L1, C7-T1, and C0-C1 joint centres. For T12-L1 and C7-T1, the joint centre was defined as the COG of the intervertebral disc elements when present, or alternatively by the local reference node at the centre of a coordinate frame representing the centre of the intervertebral disc. For C0-C1, a fixed anatomical reference point was defined at the most anterior-superior node of the dens (odontoid process). Although this point does not represent a direct anatomical joint centre of the atlanto-occipital articulation, it was chosen as a practical harmonised landmark because studies suggest dens as a nearby central rotational reference in the upper cervical complex and lies close to the anatomical rotation centre axis [27]. These joint centre definitions are pragmatic landmarks for transferring the volunteer-derived posture values to HBMs, and they are not claimed to be exact anatomical joint centres. The uncertainty introduced by these HBM joint centre definitions was not quantified in the present study and is therefore treated as a methodological limitation.

The final LMM-predicted nominal posture values were implemented in the three AM50 HBMs in VPS environment. The pelvis and spine of each complete HBM were defined in the same HJC-centred sagittal coordinate system used for the statistical posture variables. For each HBM, its own mid-HJC was treated as the local coordinate origin (X = 0, Z = 0). The HBM was rotated in the sagittal plane until the HJAS pelvis angle matched the LMM-predicted nominal pelvis angle. Next, each spinal vertebrae was articulated to reach the LMM-predicted spinal posture in the pre-processor tool. The LMM-predicted X-coordinates of T12, C7, and C0 were used as direct positioning targets. The LMM-predicted Z-coordinates were retained for evaluation but were not enforced directly. This was done to avoid artificial vertical distortion, because the three models have different segment lengths, spinal geometry, and anthropometric construction. Therefore, the final workflow enforced the pelvis angle and upper-spine anterior-posterior positioning, while using the vertical coordinates as evaluation values. The same procedure was applied independently to the three HBMs. Lastly, they were positioned using an in-house marionette-method positioning framework at Audi [22]. For THUMS, the interim offset identified from the pelvis comparison sensitivity check was applied during final positioning to account for the observed sensitivity of its sphere-fitted HJC location due to the acetabulum geometry. This correction was used as a pragmatic positioning adjustment and not as a general correction factor for all THUMS applications.

After positioning, cross-HBM consistency was quantified using the range of the achieved final values across the three positioned HBMs. This range was calculated as the difference between the maximum and minimum final value for each outcome (pelvis angle and spinal landmark coordinates). The achieved pelvis angle and HJC-centred spinal landmark coordinates were also compared with the corresponding LMM-predicted nominal values using the deviation

$$\Delta q = q_{\text{final}} - q_{\text{predicted}} \tag{7}$$

where q denotes the pelvis angle or one of the HJC-centred spinal landmark coordinates. To express the deviations relative to the variability observed in the volunteer data, each absolute deviation was normalised by the RMSE of the corresponding final LMM by

$$E_{\text{RMSE}} = \frac{|\Delta q|}{RMSE_q} \tag{8}$$

where E_{RMSE} is the RMSE-normalised deviation and $RMSE_q$ is the RMSE of the corresponding final LMM outcome q. Values with $\mathrm{E}_{\text{RMSE}} \leq 1$ were interpreted as being within the tight tolerance band, while values with $1 < \mathrm{E}_{\text{RMSE}} \leq 2$ were interpreted as being within the extended tolerance band.

III. RESULTS

Cross-model Pelvis Comparison Study and Selection of HJAS

When the five pelvis geometries were initially translated to the common local mid-HJC origin (X=0, Z=0), differences in anterior pelvis landmark alignment were observed. The HJC-translation-only baseline produced an ASIS RMS dispersion of 10.33 mm, a pubic symphysis RMS dispersion of 8.64 mm, and a combined ASIS + pubic symphysis RMS dispersion of 9.52 mm. Table 1 summarises the quantitative RMS dispersion results for the cross-model pelvis comparison study.

Table 1. Comparison of pelvis-angle definitions using sagittal-plane RMS dispersion of ASIS and pubic symphysis landmarks.

Pelvis-angle definition	ASIS RMS dispersion (mm)	Pubic symphysis RMS dispersion (mm)	Combined ASIS + pubic RMS dispersion (mm)
HJC translation only	10.33	8.64	9.52
HJAS	5.36	7.93	6.77
HJLS	10.82	9.62	10.24
SS	10.01	8.17	9.14
NPA	11.44	10.15	10.81
ASLS	12.36	10.42	11.44

HJAS pelvis angle definition produced the lowest RMS dispersion for both the ASIS (5.36 mm), pubic symphysis (7.93 mm) and combined (6.77 mm). Fig. 4 illustrates the corresponding visual alignment patterns after sagittal normalisation using each evaluated pelvis-angle definition. The HJLS and ASLS definitions, which include the L5-S1 region, showed larger visual differences in the lower-spine and anterior pelvis regions, indicating sensitivity to model-specific L5-S1 geometry. The NPA definition also did not provide consistent overlap of the anterior pelvis landmarks across the five models. SS definition produced a more comparable lower spinal alignment than HJLS, NPA, and ASLS, which is consistent with its second-best combined RMS dispersion, however, the ASIS region remained less consistently aligned with the SS definition. Among the evaluated definitions, HJAS showed the most consistent visual overlap near the ASIS region, which is consistent with the quantitative ASIS RMS dispersion result. This visual comparison supports the quantitative RMS dispersion result, in which HJAS produced the lowest ASIS RMS dispersion and the lowest combined ASIS + pubic symphysis RMS dispersion. These findings supported the use of HJAS as the candidate pelvis-angle definition.

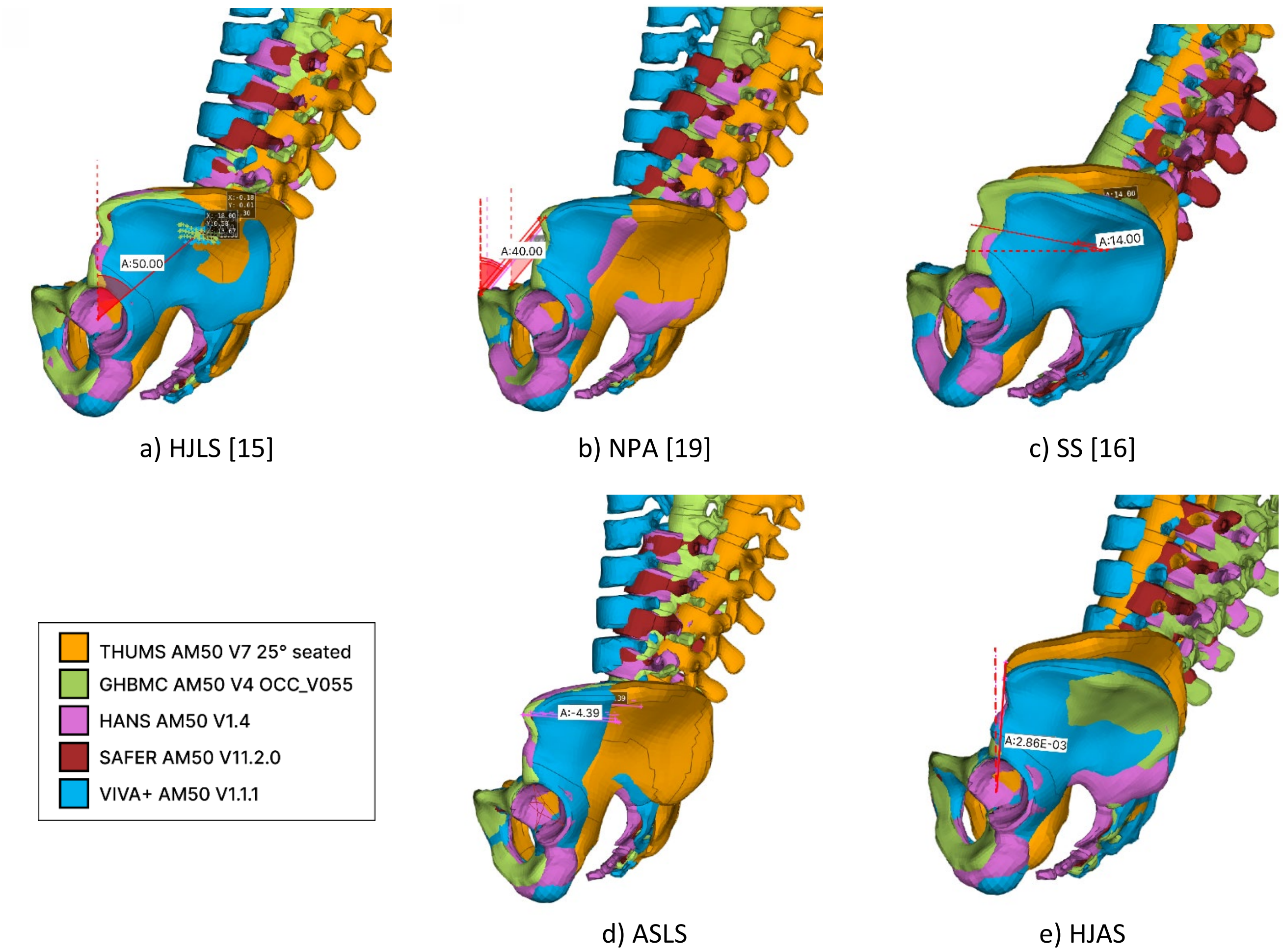

Fig. 4. Cross-model pelvis alignment after sagittal normalisation using each evaluated pelvis-angle definition: (a) HJLS, (b) NPA, (c) SS, (d) ASLS, and (e) HJAS. Each pelvis geometry was first translated to a common local mid-HJC origin and then rotated about the mid-HJC until the evaluated pelvis-angle definition reached the prescribed comparison angle. The figure provides a visual comparison of cross-model anatomical alignment.

THUMS pelvis geometry showed the largest residual difference from the other pelvis geometries for all pelvis angle definitions. This difference was quantified using the combined ASIS and pubic symphysis distance from the five-model centroid, as reported in Appendix Table A.4. Additionally, the fitted acetabulum sphere radius, calculated using the Euro NCAP HJC calculation script [3], was 35.46 mm for THUMS, whereas the corresponding radius for the other four models ranged from 26.31 to 27.89 mm. Thus, the THUMS fitted radius was approximately 30.7% larger than the mean radius of GHBMC, ViVA+, SAFER, and HANS. This supports the interpretation that differences in local acetabulum curvature influenced the sphere-fitted HJC location. A visual comparison of the acetabulum surface region used for sphere fitting is provided in Appendix Fig. A6.1, supporting the interpretation that local acetabulum curvature differed between THUMS and the other four HBMs. Hence, a pragmatic interim translation offset of 20.29 mm anteriorly and 10.83 mm inferiorly was used during the final

THUMS positioning workflow. The RMS dispersion results were calculated before applying this interim offset. Fig. 5 shows THUMS AM50 after applying this interim offset.

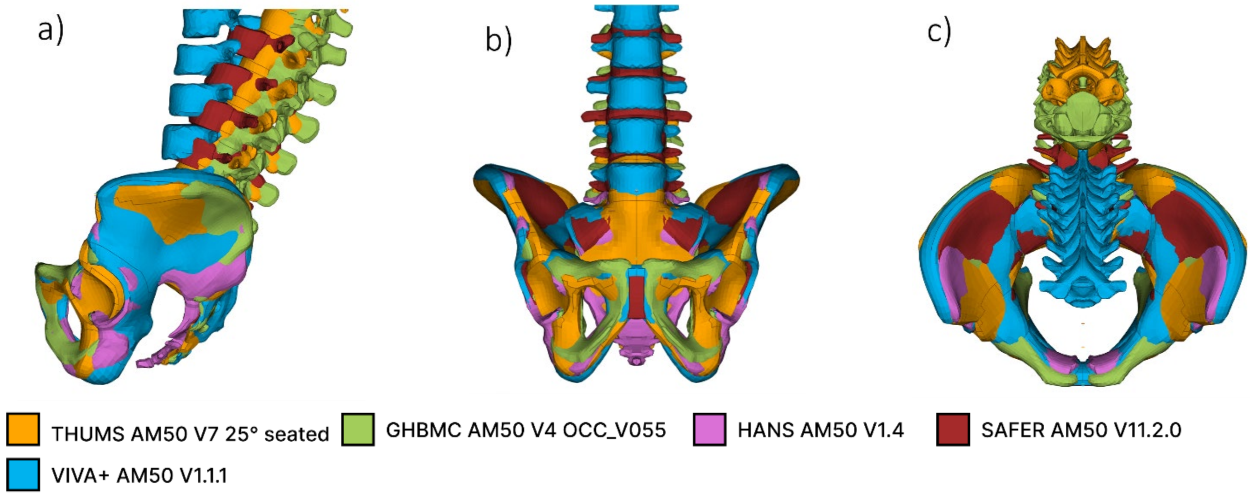

Fig. 5. Lateral (a), anterior (b), superior (c) views of the five pelvis geometries using HJAS pelvic angle definition after applying THUMS AM50 interim offsets.

Mixed-Effects Model Performance

The final reduced LMMs are summarised in Table 2. Seatback angle and headrest condition were retained in all models because they defined the seating condition. BMI, ESH, and age were retained for selected upper-spine outcomes, while gender was retained only for pelvis angle. RMSE and MAE were calculated from residuals between the observed volunteer posture values and the population-average fixed-effect predictions. They were not calculated from averaged coefficients or subject-specific random-effect predictions. Diagnostic plots (observed versus predicted values, residuals versus fitted values; Appendix Fig. A3.1-A3.7 did not indicate strong non-linear trends, supporting the use of linear models over the studied recline range. Shapiro-Wilk diagnostics [26] based on deviations from the fixed-effect predictions showed no strong evidence against normality for T12_X and T12_Z, whereas the remaining outcomes showed departures from normality (Appendix Table A.1).

The AIC/BIC comparison supported the reduced LMMs for all seven outcomes, as reported in Appendix Table A.3. For each outcome, the reduced model had lower AIC than the corresponding full model, supporting the reduced model selection based on the defined AIC criterion. BIC showed the same trend for all seven outcomes, providing supplementary support for the reduced models.

The RMSE values were 10.99° for pelvis angle and ranged from 17.64 mm to 34.11 mm for the spinal landmark coordinates. These errors reflect residual volunteer posture variability, landmark-estimation uncertainty, and model error. Therefore, the RMSE values were interpreted as practical engineering tolerance bands around the LMM-predicted nominal posture values rather than as exact normal-theory coverage limits.

Table 2. Fixed-effect coefficients and model performance of the final reduced LMMs for HJAS pelvis angle and HJC-centred spinal landmark coordinates.

Outcome	Intercept	Seatback Angle (deg)	Headrest	Age (yrs)	BMI (kg/m²)	ESH	Gender	RMSE	MAE
HJAS Pelvis_Angle (deg)	-1.66	0.44	-4.00	-	-	-	7.24	10.99	8.40
T12_X (mm)	80.92	2.60	0.80	-	-	-	-	18.71	14.58
T12_Z (mm)	278.71	-2.56	0.36	-	-	-	-	17.64	14.19
C7_X (mm)	-219.73	6.67	19.63	0.42	-2.20	0.32	-	25.26	17.33
C7_Z (mm)	12.75	-4.23	-8.49	-	2.54	0.58	-	21.76	16.74
C0_X (mm)	-276.64	8.11	52.29	0.55	-2.41	0.34	-	34.11	24.47
C0_Z (mm)	50.00	-4.96	-18.64	-	-	0.78	-	27.53	21.90

Dashes (-) indicate that the corresponding predictor was not retained in the reduced equation. Headrest was coded as 1 = "with headrest" and 0 = "without headrest"; gender was coded as 1 = "male" and 0 = "female".

For the selected AM50 input set used in the final positioning demonstration following nominal posture values were predicted: Pelvis_Angle = 15.70°, T12_X = 140.72 mm, T12_Z = 219.83 mm, C7_X = 181.20 mm, C7_Z =

496.94 mm, C0_X = 175.12 mm, and C0_Z = 632.85 mm. The corresponding HJC-centred nominal upper-spine posture is shown in Fig. 6.

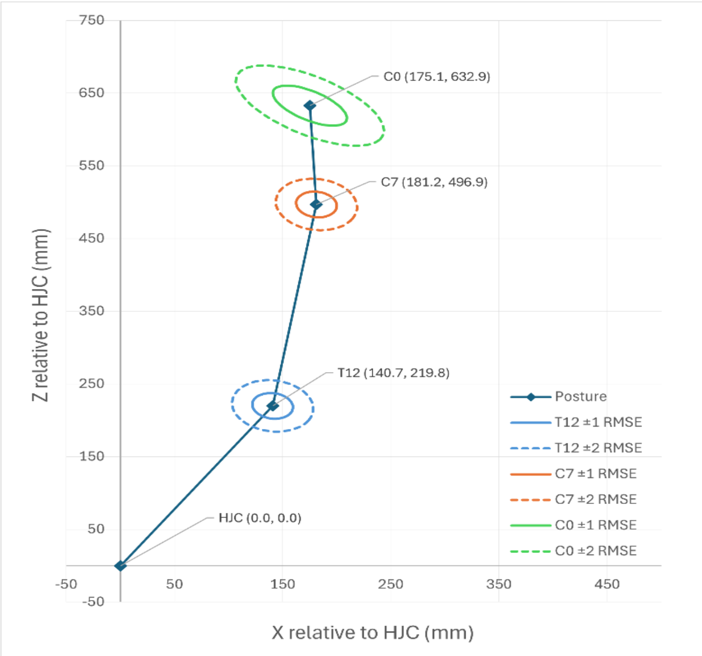

Fig. 6. HJC-centred spine T12-L1, C7-T1, and C0-C1 landmarks predicted by the final reduced LMMs for a male, age 39 years, BMI 24.9 kg/m², ESH 893.5 mm, seatback angle 23°, and without headrest.

Application to Three Available AM50 HBMs for Marionette Positioning

The positioned THUMS, GHBMC, and ViVA+ postures were compared with the corresponding LMM-predicted nominal pelvis angle and HJC-centred spinal landmark coordinates. Fig. 7 shows the final positioned models. The corresponding original and newlypositioned posture comparisons for each implemented HBM are provided in Appendix Fig. A2.1-A2.3. Across the three HBMs, the final HJAS pelvis angles ranged from 14.976° to 15.002°, corresponding to a cross-model range of 0.02° and a maximum absolute deviation of 0.72° from the LMM-predicted value of 15.70°.

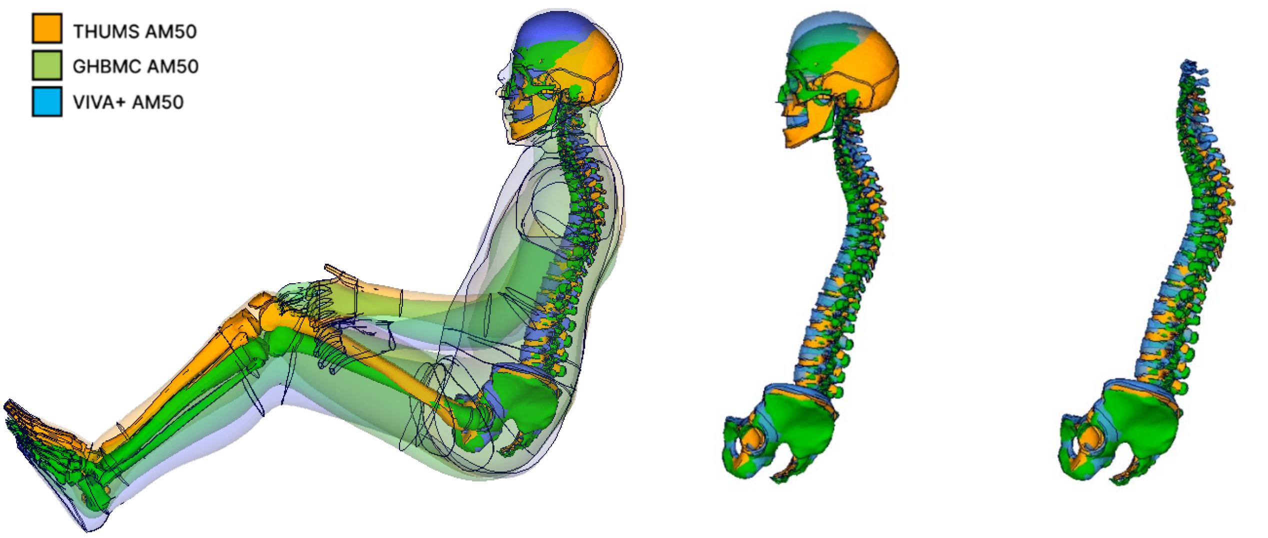

a) Full body b) Pelvis spine and skull c) Pelvis and spine

Fig. 7. Positioned postures of THUMS AM50, GHBMC M50, and ViVA+ 50M.

Table 3 summarises the cross-HBM consistency of the final positioned postures and the corresponding deviations from the LMM-predicted nominal posture values. The final HJAS pelvis angle showed a very small cross-HBM spread of 0.03°, indicating consistent pelvis orientation across THUMS, GHBMC, and ViVA+. For the enforced anterior-posterior spinal coordinates, the cross-HBM spreads were 2.87 mm for T12_X, 4.79 mm for C7_X, and

3.35 mm for C0_X. These values indicate that the three HBMs were positioned consistently in the anterior-posterior direction. Larger cross-HBM spreads were observed for the vertical coordinates, particularly C7_Z and C0_Z, which were evaluated but not directly enforced during positioning. The maximum RMSE-normalised deviations were 1.24 for T12_Z, 1.22 for C7_Z, and 0.93 for C0_Z. Overall, 19 of the 21 evaluated pelvis and spinal quantities were within ±1×RMSE, and all 21 were within ±2×RMSE.

Table 3. Cross-HBM consistency and deviation from LMM-predicted nominal posture values after positioning.

Quantity	LMM Predicted value	Range across positioned HBMs	Cross-HBM spread	Max. absolute deviation	Max. deviation / RMSE
HJAS Pelvis_Angle (deg)	15.70°	14.98 - 15.00	0.03	0.72	0.07
T12_X (mm)	140.72	146.11 - 148.98	2.87	8.26	0.44
T12_Z (mm)	219.83	217.46 - 241.69	24.23	21.86	1.24
C7_X (mm)	181.20	185.10 - 189.89	4.79	8.69	0.34
C7_Z (mm)	496.94	484.70 - 523.47	38.77	26.53	1.22
C0_X (mm)	175.12	181.68 - 185.03	3.35	9.91	0.29
C0_Z (mm)	632.85	607.11 - 651.67	44.56	25.74	0.94

Pelvis angle and coordinates are expressed in the HJC-centred sagittal coordinate system. Cross-HBM spread was calculated as the maximum final value minus the minimum final value across THUMS, GHBMC, and ViVA+.

IV. DISCUSSION

This study proposes an anatomy-based procedure for harmonised initial pelvis and upper-spine positioning of AM50 HBMs. The main contributions are threefold. First, the cross-model pelvis comparison showed that the HJAS pelvis-angle definition produced the lowest RMS dispersion of the pelvis landmarks, namely ASIS and pubic symphysis, among the evaluated pelvis-angle definitions. This supports the use of HJAS as the candidate pelvis-angle definition for the present positioning workflow, while the iliac crest was retained only as a supporting visual/anatomical reference. Second, HJC-centred LMMs were developed to estimate nominal pelvis angle and upper-spine landmark positions at T12-L1, C7-T1, and C0-C1 from volunteer posture data. Third, the resulting LMM-predicted nominal values were implemented in a marionette- method based positioning workflow and evaluated quantitatively with three HBMs in VPS simulation environment. The procedure is intended to improve consistency of initial posture definition across HBMs, not to demonstrate improved crash-response prediction or optimized restraint interaction.

Current Euro NCAP's virtual testing procedures specify target seat and HJC positions but do not prescribe a unified pelvis and spine posture [3]. In the absence of such guidance, different users may position HBMs based on internal practices or subjective visual judgements, which complicates comparisons across studies and between different HBMs. The present guideline could extend the positioning procedure used in CP-551 by standardising pelvis angle definition (HJAS) and spine positioning via LMM, along with nominal T12-L1, C7-T1 and C0-C1 nominal positions with explicit tolerances based on volunteer variability [3]. This would allow more consistent initial posture definitions across multiple HBMs, in the same seated configuration.

This harmonization should be interpreted as a standardisation strategy for model comparability, not as a claim that one pelvis and spine posture represent all AM50 occupants. Differences in pelvis orientation and spinal curvature across humans can reflect genuine subject-specific anatomy, comfort preferences, and seating behavior [15–17]. Enforcing a common nominal posture may therefore reduce subject-specific realism, although it improves the comparability of simulations performed with different HBMs. This trade-off is inherent to the proposed workflow: The method aims to reduce avoidable user and model dependent differences in initial posture, specifically for the pelvis and spine, while residual human posture variability is represented only indirectly through the RMSE-based tolerance bands.Additionally, it was found out in a section view with all the pelvis geometries aligned during the cross-HBM pelvis comparison that the L5-S1 joint varies greatly across models. This observation is consistent with the morphometric variability in sacral and pelvic geometry reported by Brynskog and colleagues [28]. Hence, in this study the L5-S1 joint was excluded for defining the spinal posture.

The Reed and Ebert dataset was selected as the primary statistical source because it provided individual-level automotive passenger-posture data across multiple seatback angles and headrest conditions, together with the landmark and anthropometric variables required to construct the HJC-centred pelvis and upper-spine posture representation [15]. Other published datasets were considered, including imaging-based and volunteer-posture studies; however, comparable individual-level data with the required combination of HJC, ASIS, T12-L1, C7-T1, and C0-C1 landmarks were not available to the authors at the time of analysis, or different seat type was used, or posture and landmark definitions that were not directly compatible with the present workflow [14][16][17][20]. However, a key limitation is that the Reed and Ebert dataset was obtained using one passenger-seat mock-up configuration, one fixed seat pan angle, and four tested seatback angles [15]. Therefore, the LMM-predicted nominal posture values should not be interpreted as universally valid for all seat designs, belt geometries, seat pan angles, or extreme recline configurations. Extrapolation to other seat designs or more extreme reclines should be done cautiously. In addition, the source data rely on palpated surface landmarks, flesh-margin corrections, and regression/optimization-derived skeletal joint centres rather than direct imaging of all skeletal landmarks [15]. These factors introduce uncertainty when volunteer-derived pelvis and spine posture values are transferred to HBM landmark definitions.

The conclusion that HJAS provided the most consistent alignment is limited to the ASIS and pubic symphysis landmarks evaluated in this study. It should not be interpreted as complete pelvis-surface alignment or quantitative iliac-crest alignment. In addition, the cross-model pelvis comparison was performed in a local HJC-centred coordinate system and did not evaluate the influence of vehicle-specific HBM placement using the full Euro NCAP CP-551/Frontal_VTC procedure [3]. Therefore, possible effects of seat geometry, vehicle interior measurements, and model-specific anthropometric inputs on the HBM Pelvis X- and Z-location in the global vehicle coordinate system were outside the scope of this study and should be assessed in future complete-vehicle positioning studies. Because abdominal and thigh soft-tissue geometry was not included in the cross-model pelvis comparison, the RMS-dispersion results should not be interpreted as quantifying belt-pelvis engagement, submarining risk, or abdominal loading [11][13].

The current implementation uses one common nominal AM50 input set for demonstration purposes. To assess the influence of HBM-specific anthropometric inputs, a supplementary sensitivity check was performed for a reference seating condition with 23° seat-back angle, without headrest, male gender, and age kept constant (39 years), while BMI and ESH were varied using HBM-specific values for THUMS, GHBMC, and ViVA+. The BMI and ESH input pairs were 25.14 kg/m² and 910.00 mm for THUMS, 25.69 kg/m² and 909.48 mm for GHBMC, and 25.00 kg/m² and 911.56 mm for ViVA+ [5–6][29]. ESH was estimated as 0.52 times stature. The predicted pelvis angle and T12_X and T12_Z nominal values remained unchanged across the three cases. For the upper-spine landmarks, the maximum variation across the three input sets was 2.18 mm for C7_X, 1.09 mm for C7_Z, 2.37 mm for C0_X, and 1.62 mm for C0_Z. These differences were comparatively smaller than the corresponding RMSE values of the reduced LMMs, indicating limited sensitivity of nominal posture values to plausible HBM-specific BMI and ESH variation for the tested reference condition. The corresponding predicted nominal values are summarised in Appendix Table A.2.

A further limitation is that AM50 HBMs are not identical representations of one standardised human subject. They differ in source anthropometry, segmentation strategy, mesh topology, pelvis morphology, spinal geometry, soft-tissue distribution, and developer-specific modelling choices [4–7][21]. Therefore, some residual differences after applying a harmonised positioning procedure are expected and should not be interpreted as positioning errors alone. The present workflow reduces avoidable differences in the definition of initial posture, but it cannot remove all anatomical and structural differences between HBMs. The interim THUMS translation offset used in the final positioning workflow should therefore be interpreted as a pragmatic adjustment for the present implementation, based on the observed sensitivity of the sphere-fitted HJC to local acetabulum geometry. It should not be interpreted as a universal correction factor for THUMS or as evidence of an error in any HBM until further studied.

The final marionette-method based implementation was limited to THUMS AM50, GHBMC M50, and ViVA+ 50M because complete models were available for these HBMs in VPS environment. HANS and SAFER were included in the pelvis-angle comparison using available pelvis and lumbar-spine geometries, but complete models were not available for final positioning. Therefore, the final three-model implementation should not be interpreted as a selection based on more favourable alignment behaviour.

The upper-body posture was represented using three HJC-centred landmarks, T12-L1, C7-T1, and C0-C1, rather than a full vertebra-level curvature description. This was sufficient for defining a compact thorax, neck, and head positioning workflow, but it does not prescribe individual vertebral rotations or detailed lumbar curvature. In addition, the HBM landmark definitions used to transfer volunteer-derived joint locations to THUMS, GHBMC, and ViVA+ are pragmatic harmonised definitions, not direct anatomical measurements. For T12-L1 and C7-T1, disc centres or local reference frames were used when available, while C0-C1 was represented using a practical upper-cervical reference point near the dens. The uncertainty introduced by these HBM landmark definitions was not quantified in the present study and should be evaluated in future work using imaging-based datasets or other independent anatomical references. The final quantitative positioning assessment was limited to pelvis angle and selected HJC-centred spinal landmarks. Lower-limb and femur orientation changes were not quantified in the present study. These quantities should be evaluated in future work, particularly if the workflow is applied in full crash simulations where femur orientation, knee position, and lower-limb interaction with the restraint and interior may influence occupant kinematics.

Finally, the present study evaluated geometric posture harmonization, not crash-response validation. The results do not demonstrate improved injury prediction, submarining prediction, or equivalence of dynamic response across HBMs. Full frontal crash simulations are required to evaluate whether the harmonised initial posture affects occupant kinematics, belt-pelvis interaction, submarining risk, and injury-related metrics.

Future work should include applying the proposed workflow in full frontal crash simulations with different HBMs to evaluate its influence on occupant kinematics, belt-pelvis interaction, submarining risk, and injury-related metrics. Additional volunteer and imaging-based datasets should be used to supplement or validate the Reed and Ebert-based posture predictions and to quantify the uncertainty introduced by transferring human landmark estimates to HBM landmark definitions. The approach should also be extended to additional body sizes and populations and to other seat designs, seat pan angles, belt geometries, and reclined seating configurations. Finally, the current three-landmark spine representation could be refined by incorporating vertebra-level curvature, segment rotations, and lower-limb/femur orientation metrics.

V. CONCLUSION

This study developed a candidate anatomy-based workflow for harmonised initial pelvis and upper-spine positioning which was tested with AM50 HBMs. A pelvis-angle definition based on the HJC and ASIS (HJAS) produced the lowest combined ASIS + pubic symphysis RMS dispersion across the five HBM pelvis geometries and was therefore selected as the candidate pelvis-angle definition for the present workflow. In addition, LMMs derived from the Reed and Ebert 2018 reclined-posture dataset were used to predict nominal pelvis angle and HJC-centred based spinal joint centres namely T12-L1, C7-T1, and C0-C1 as functions of seat-back angle, headrest use, and selected anthropometric variables. When implemented in THUMS, GHBMC, and ViVA+ in VPS simulation environment, the workflow produced quantitatively comparable initial postures, with 19 of 21 evaluated pelvis and spinal quantities within ±1×RMSE and all evaluated quantities within ±2×RMSE. The procedure should therefore be interpreted as a practical approach for improving consistency of nominal initial posture definition across HBMs, not as a universal posture standard or as evidence of improved crash-response prediction. Future work should evaluate the workflow in crash simulations, additional HBMs, other body sizes, and further volunteer or imaging-based datasets.

VI. ACKNOWLEDGEMENTS

The author gratefully acknowledges AUDI AG, Ingolstadt, for supporting this work. The author sincerely thanks Prof. Matthew P. Reed (UMTRI) for providing access to the individual-level volunteer dataset and for his valuable advice on the statistical methodology. Appreciation is further extended to the ViVA+ consortium and to Ansys, Chalmers University of Technology, and Volvo Cars for providing pelvis geometry that supported the comparative analyses. Special thanks are extended to Prof. Dr.-Ing. Daniel Juhre and Dr.-Ing. Sascha Eisenträger at Otto-von-Guericke University Magdeburg for their guidance and support throughout this study.

VII. REFERENCES

1. European Commission. Position and Personalize Advanced Human Body Models for Injury Prediction (PIPER): FP7 Project 605544. 2013. https://cordis.europa.eu/project/id/605544. Accessed 13 Feb 2026.
2. Euro NCAP. CP-550 Qualification Procedure for Human Body Models. https://www.euroncap.com/media/87114/cp-550-hbm-qualification-v09.pdf. Accessed 4 Feb 2026.
3. Euro NCAP. CP-551 Human Body Model Simulations in Frontal Impacts. https://www.euroncap.com/media/95016/cp-551-human-body-model-simulations-in-frontal-impacts-v11.pdf. Accessed 4 Feb 2026.
4. John J, Klug C, Kranjec M, Svenning E, Iraeus J. Hello, world! VIVA+: A human body model lineup to evaluate sex-differences in crash protection. Front Bioeng Biotechnol. 2022;10:918904. doi:10.3389/fbioe.2022.918904.
5. Iwamoto M, Nakahira Y, Kimpara H. Development and Validation of the Total HUman Model for Safety

(THUMS) Toward Further Understanding of Occupant Injury Mechanisms in Precrash and During Crash. Traffic Inj Prev. 2015;16 Suppl 1:S36-48. doi:10.1080/15389588.2015.1015000.
6. F. Scott Gayzik, Daniel P. Moreno, Nicholas A. Vavalle. Development of the global human body models consortium mid-sized male full body model; 2011.
7. Pipkorn B, Jakobsson L, Iraeus J, Östh J. THE SAFER HBM-A human body model for seamless integrated occupant analysis for all road users.
8. Toyota Motor Corporation. THUMS – About. https://www.toyota.co.jp/thums/about. Accessed 14 Feb 2026.
9. Global Human Body Models Consortium (GHBMC). GHBMC – Global Human Body Models Consortium. https://www.ghbmc.com/. Accessed 14 Feb 2026.
10. Nishida N, Izumiyama T, Asahi R, Jiang F, Ohgi J, Yamagata H, et al. Analysis of individual differences in pelvic and spine alignment in seated posture and impact on the seatbelt kinematics using human body model. PLoS One. 2021;16:e0254120. doi:10.1371/journal.pone.0254120.
11. Richardson Rachel, Jayathirtha Mohan, Donlon J. P. ,Forman Jason L., Gepner – Brian, Östling Mats, Mroz Katarzyna, Pipkorn Bengt, Kerrigan J. R. / Jason R. Pelvis kinematics and injuries of reclined occupants in frontal impacts. In: 2020 IRCOBI Conference Proceedings. p. 499–515.
12. Tanaka Y, Takeuchi Y, Zhao Y, Yang N, Mizuno K, Tanaka Y, Hosokawa N. FE Analyses of the Lap Belt Interactions With the Pelvis for Diverse Occupants in Various Sitting Postures. In: 27th International Technical Conference on the Enhanced Safety of Vehicles (ESV): National Highway Traffic Safety Administration (NHTSA); 2023. p. 1–16.
13. Naseri H, Iraeus J, Johansson H. A numerical study on the safety belt-to-pelvis interaction. Int J Numer Method Biomed Eng. 2022;38:e3572. doi:10.1002/cnm.3572.
14. Tanaka Y, Nakashima A, Feng H, Mizuno K, Yamada M, Yamada Y, et al. Analysis of Lap Belt Fit to Human Subjects using CT Images. Stapp Car Crash J. 2021;65:49–90. doi:10.4271/2021-22-0004.
15. Reed MP, Ebert SM. Effects of recline on passenger posture and belt fit. September / 2018. https://deepblue.lib.umich.edu/bitstream/2027.42/146263/1/UMTRI-2018-2 .pdf.
16. Izumiyama T, Nishida N, Yamagata H, Asahi R, Chen X, Ohgi J, et al. Analysis of individual variabilities for lumbar and pelvic alignment in highly reclined seating postures and occupant kinematics in a collision. In: ; 2022. p. 941–955.
17. Grébonval C, Beillas P, Wang X. Experimental investigation of preferred seating positions and postures in reclined seating configurations. In: ; 2021. 6p.
18. Reed MP. Statistical and biomechanical prediction of automobile driving posture: University of Michigan; 1998.
19. Nyquist GW, Patrick LM. Lumbar and pelvic orientations of the vehicle seated volunteer. SAE Transactions. 1976:2610–21.
20. Forman J, Booth G, Mergler O, Romani S, Zhang H, Roberts C, et al. Variability in Body Shape, Superficial Soft Tissue Geometry, and Seatbelt Fit Relative to the Pelvis in Automotive Postures-Methods for Volunteer Data Collection With Open Magnetic Resonance Imaging. J Biomech Eng 2024. doi:10.1115/1.4064477.
21. Benito Cia L. HANS meets the GNS software: Working with HBMs in Generator4 and Animator4. In: 2024 International LS-DYNA Conference (Metro Detroit, Michigan, USA).
22. David Poulard, Damien Subit, John-Paul Donlon, Richard W. Kent. Development of a computational framework to adjust the pre-impact spine posture of a whole-body model based on cadaver tests data. J Biomech. 2015;48:636–43. doi:10.1016/j.jbiomech.2014.12.050.
23. Sheeran L, Hemming R, van Deursen R, Sparkes V. Can different seating aids influence a sitting posture in healthy individuals and does gender matter? Cogent Engineering. 2018;5:1442109. doi:10.1080/23311916.2018.1442109.
24. Bates D, Mächler M, Bolker B, Walker S. Fitting Linear Mixed-Effects Models Using lme4 2015. doi:10.18637/jss.v067.i01.
25. Burnham KP, Anderson DR. Multimodel Inference. Sociological Methods & Research. 2004;33:261–304. doi:10.1177/0049124104268644.
26. SHAPIRO SS, WILK MB. An analysis of variance test for normality (complete samples). Biometrika. 1965;52:591–611. doi:10.1093/biomet/52.3-4.591.

27. Roche CJ, King SJ, Dangerfield PH, Carty HM. The atlanto-axial joint: physiological range of rotation on MRI and CT. Clin Radiol. 2002;57:103–8. doi:10.1053/crad.2001.0703.
28. Brynskog E, Iraeus J, Reed MP, Davidsson J. Predicting pelvis geometry using a morphometric model with overall anthropometric variables. J Biomech. 2021;126:110633. doi:10.1016/j.jbiomech.2021.110633.
29. VIVA+ Team. Anthropometry -- VIVA+ Human Body Models: Online model documentation. 2025. https://vivaplus.readthedocs.io/en/latest/model/anthro/. Accessed 25 Mar 2026.

VIII. APPENDIX

Appendix A.1: Overview of AM50 HBMs considered in the study

a) THUMS AM50

b) HANS AM50

c) GHBMC M50-O

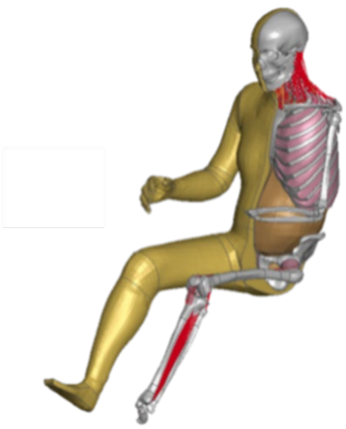

d) ViVA+ 50M

e) SAFER AM50

Fig. A1.1 Five AM50 HBMs considered in this study [7–9][21][29]

Appendix A.2: Original initial posture and guideline-positioned posture comparison for THUMS AM50, GHBMC M50, and VIVA+ 50M

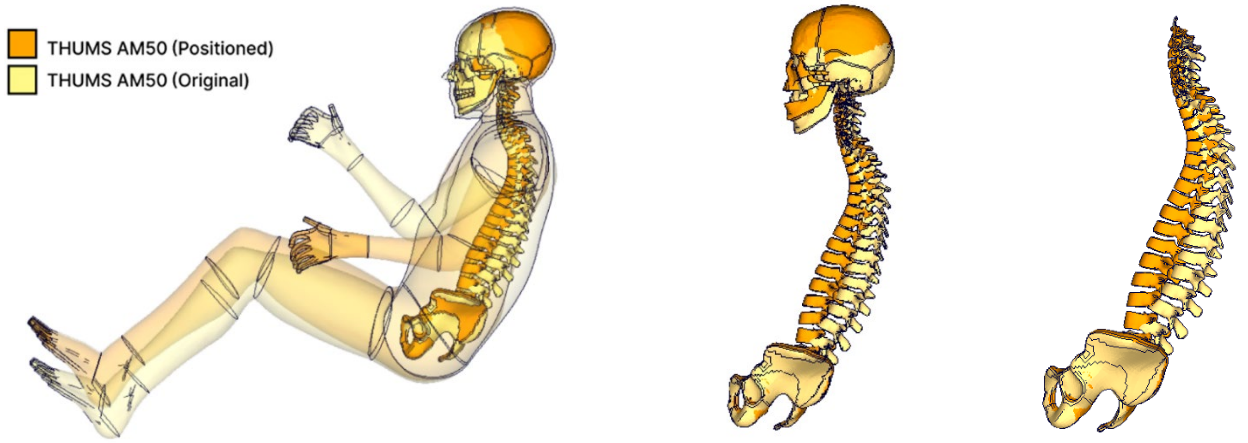

a) Full Specimen b) Pelvis, spine, and skull c) Pelvis and spine

Fig. A2.1 Visual comparison of the original and guideline-positioned posture of THUMS AM50.

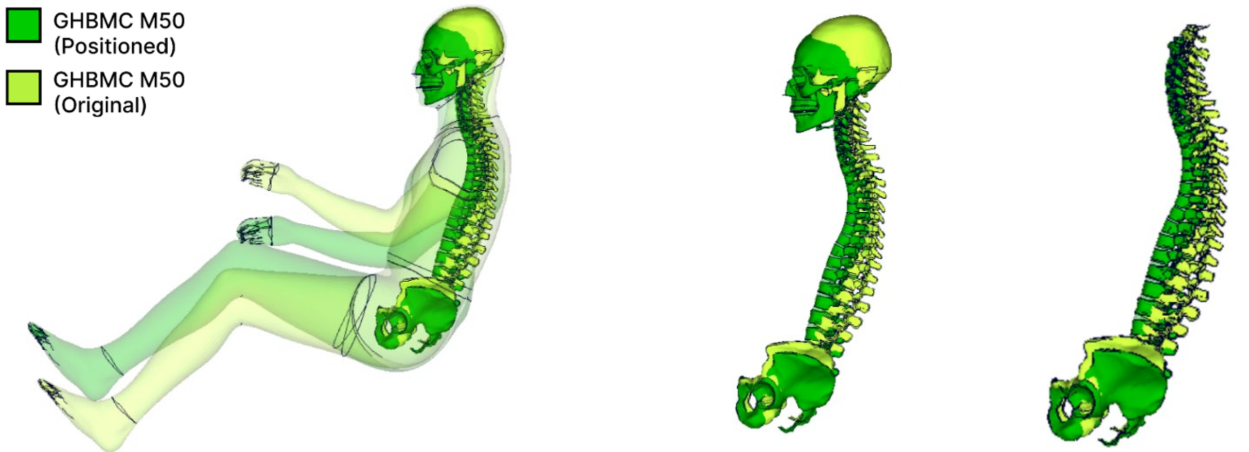

d) Full Specimen e) Pelvis, spine, and skull f) Pelvis and spine

Fig. A2.2 Visual comparison of the original and guideline-positioned posture of GHBMC M50.

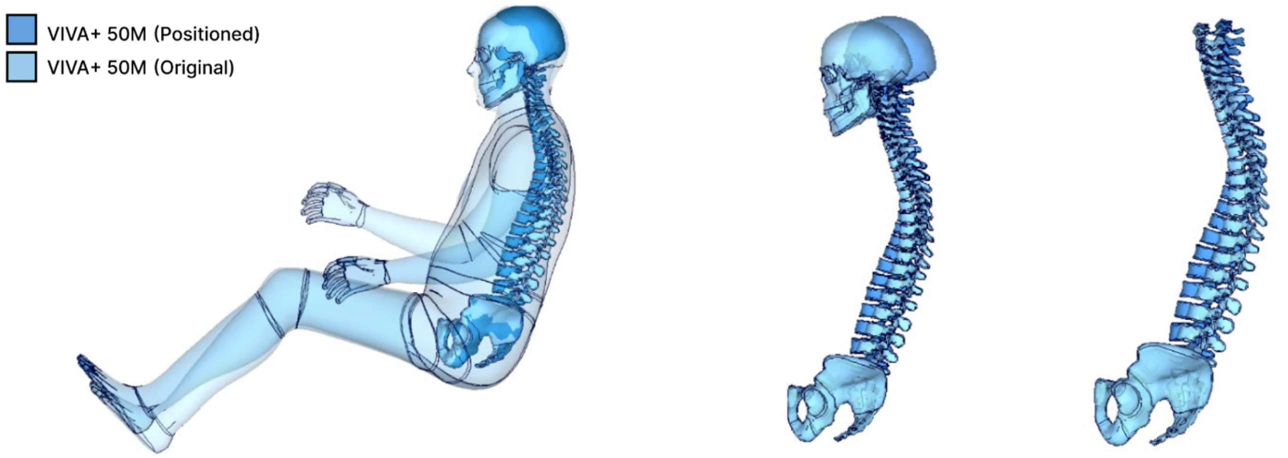

g) Full Specimen h) Pelvis, spine, and skull i) Pelvis and spine

Fig. A2.3 Visual comparison of the original and guideline-positioned posture of ViVA+ 50M.

Appendix A.3: Diagnostic plots for reduced LMMs

The diagnostic graphs for the reduced LMMs used to predict the spinal landmark coordinates and pelvic angle are displayed in this appendix. Residual-versus-predicted plot displays the distribution of residuals across the prediction range for each outcome, whereas an observed-versus-predicted plot shows the agreement between the measured values and the population-average (fixed-effects) predictions. These plots were used to confirm that there are no significant systematic trends left in the residuals and that the models adequately describe the posture data.

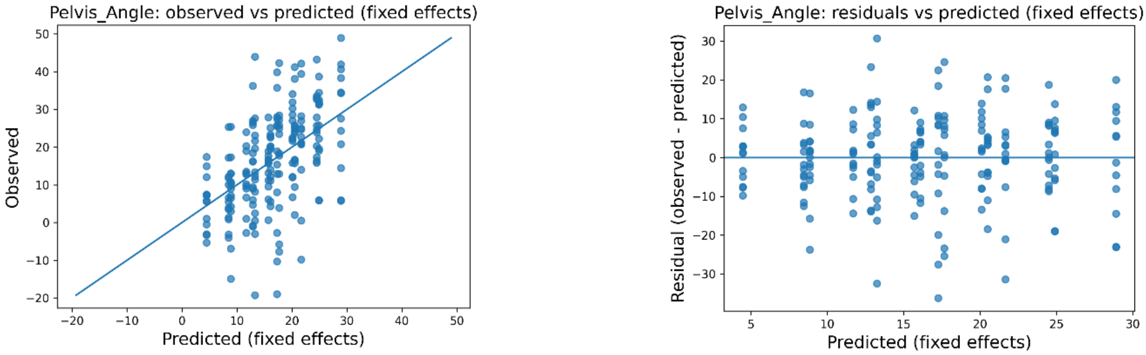

Fig. A3.1 Diagnostic plots for the reduced LMM of Pelvis_Angle

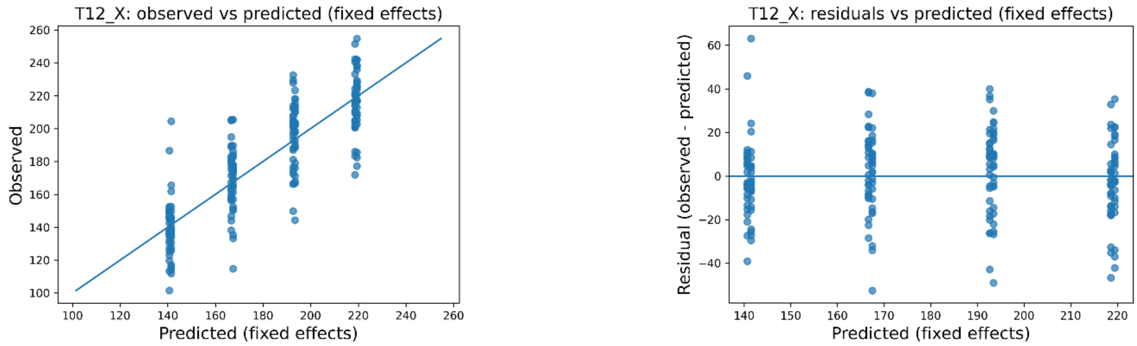

Fig. A3.2 Diagnostic plots for the reduced LMM of T12_X.

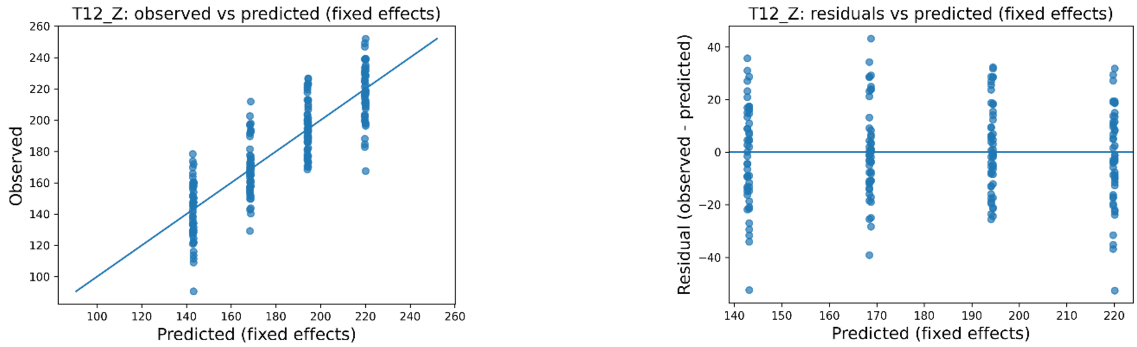

Fig. A3.3 Diagnostic plots for the reduced LMM of T12_Z.

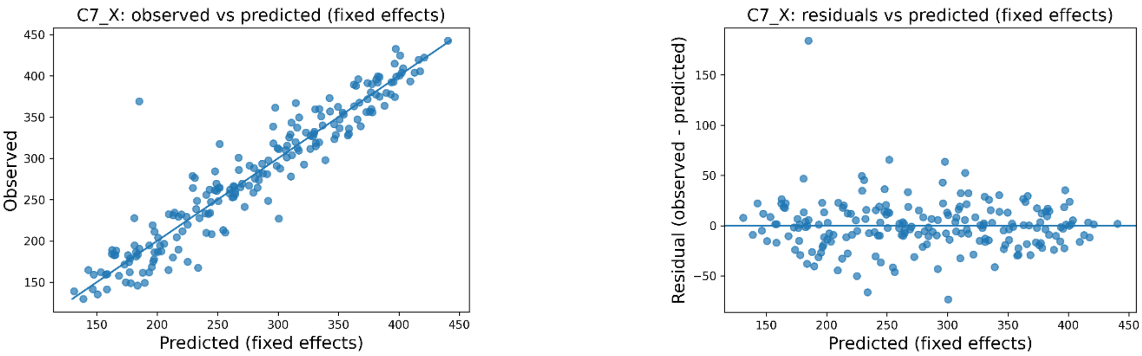

Fig. A3.4 Diagnostic plots for the reduced LMM of C7_X.

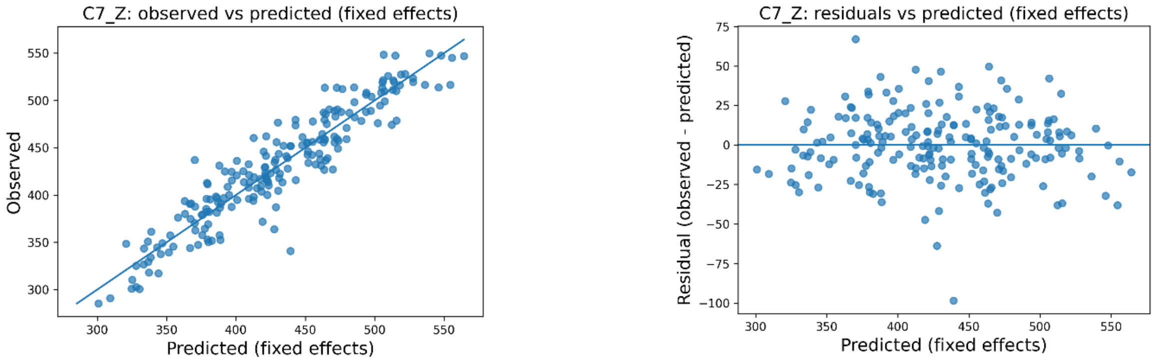

Fig. A3.5 Diagnostic plots for the reduced LMM of C7_Z.

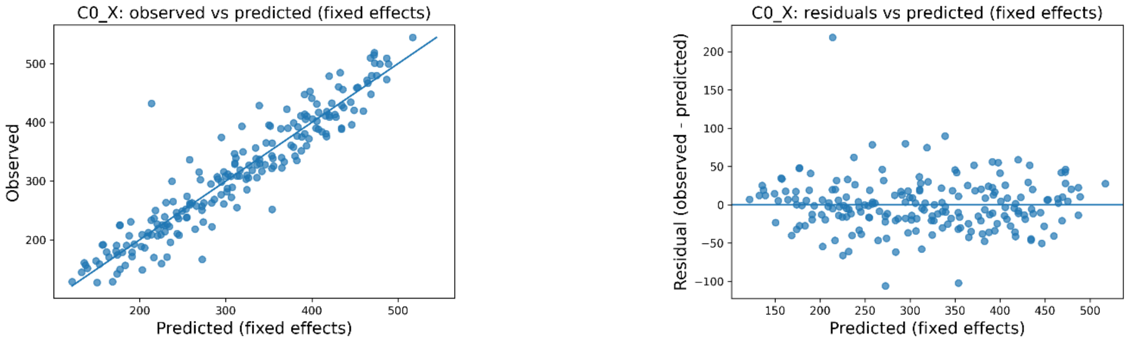

Fig. A3.6 Diagnostic plots for the reduced LMM of C0_X.

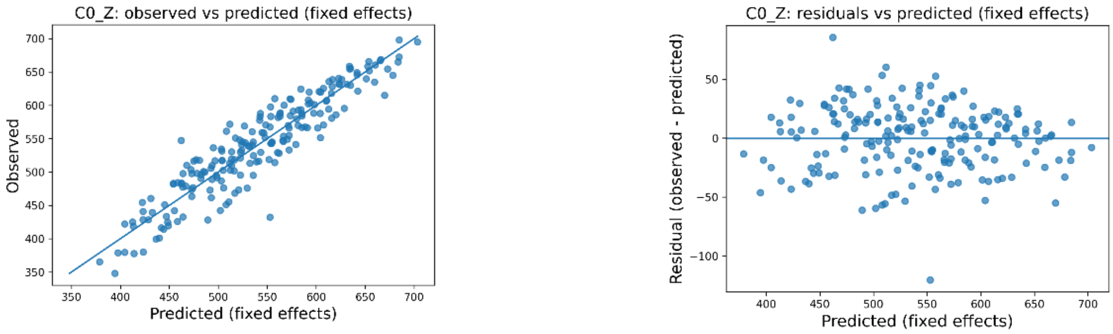

Fig. A3.7 Diagnostic plots for the reduced LMM of C0_Z.

Appendix A.4: Residual normality diagnostics for final reduced LMMs.

Residual normality for deviations from the fixed-effect predictions was assessed using the Shapiro-Wilk test [26], and the results are summarised in the table below.

Table A.1 Residual normality diagnostics for the final reduced LMMs based on deviations from the fixed-effect predictions.

Outcome	N	Shapiro-Wilk W	p-value	Interpretation
HJAS Pelvis_Angle (deg)	200	0.9838	0.0213	Departure from normality.
T12_X (mm)	200	0.9920	0.3384	No strong evidence against normality.
T12_Z (mm)	200	0.9925	0.3944	No strong evidence against normality.
C7_X (mm)	200	0.8845	2.88e-11	Departure from normality.
C7_Z (mm)	200	0.9832	0.0171	Departure from normality.
C0_X (mm)	200	0.9224	8.73e-09	Departure from normality.
C0_Z (mm)	200	0.9807	0.00747	Departure from normality.

N denotes the number of residual observations used in the residual-normality assessment.

Appendix A.5: Sensitivity check for HBM-specific BMI and ESH inputs

A supplementary sensitivity check was performed for the 23° reference seating condition to assess the influence of HBM-specific BMI and ESH inputs on the reduced LMM nominal posture predictions. Seat-back angle, headrest condition, sex, and age were kept constant (23°, None, male, 39 years). The BMI, and ESH input pairs were 25.14 kg/m² and 910.00 mm for THUMS, 25.69 kg/m² and 909.48 mm for GHBMC, and 25.00 kg/m² and 911.56 mm for ViVA+, with ESH estimated as 0.52 times the stature based on the Euro NCAP CP-551v1.1. Pelvis angle, T12_X, and T12_Z values were unchanged across the three cases. The maximum variation was 2.18 mm for C7_X, 1.09 mm for C7_Z, 2.37 mm for C0_X, and 1.62 mm for C0_Z [4–9][29][3].

Table A.2 Reduced LMM nominal posture predictions for HBM-specific BMI and ESH.

Predicted Joint Centres	THUMS	GHBMC	ViVA+
HJAS Pelvis_Angle (deg)	15.70	15.70	15.70
T12_X (mm)	140.72	140.72	140.72
T12_Z (mm)	219.83	219.83	219.83
C7_X (mm)	185.95	184.58	186.76
C7_Z (mm)	507.12	508.21	507.66
C0_X (mm)	180.15	178.65	181.02
C0_Z (mm)	645.72	645.31	646.93

Appendix A.6: Acetabulum Geometry Check for Sphere-Based HJC Estimation

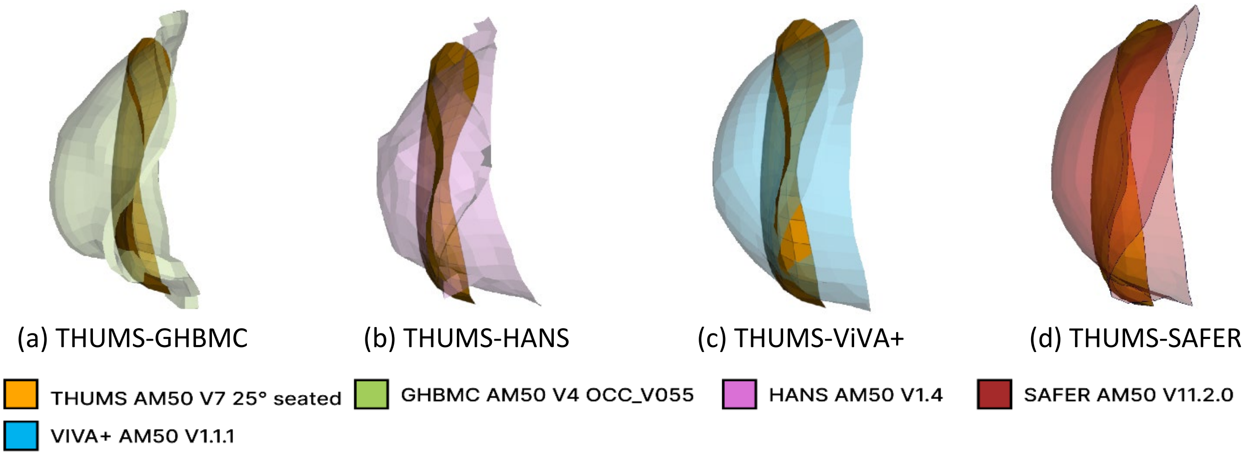

Fig. A6.1 Comparison of the acetabulum surface region used for sphere-based HJC estimation: (a) THUMS-GHBMC, (b) THUMS-HANS, (c) THUMS-ViVA+, and (d) THUMS-SAFER. The figure is provided as visual support for the fitted-radius sensitivity check.

Quantitative interpretation was based on the fitted acetabulum sphere radii, where THUMS showed a larger fitted radius than the other evaluated models. This indicates a difference in local acetabulum curvature affecting sphere-based HJC estimation, not an error or deficiency in any HBM.

Appendix A.7: AIC/BIC Comparison for Final Reduced LMM Selection

A supplementary BIC check was performed for the final LMM selection. For each outcome, the full LMM included seatback angle, headrest condition, age, BMI, ESH, and gender as fixed effects, with a random intercept and random seatback-angle slope per subject. A reduced model was then fitted using the same predictor-selection logic described in the Methods section. The comparison was calculated as $\Delta AIC = AIC_{reduced} - AIC_{full}$ and $\Delta BIC = BIC_{reduced} - BIC_{full}$. Negative ΔAIC or ΔBIC values indicate that the reduced model had a lower information criterion value than the corresponding full model [25]. BIC supported the same model-selection direction as AIC for all seven outcomes.

Table A.3 AIC and BIC comparison between full and reduced LMMs for pelvis angle and HJC-centred spinal landmark coordinates.

Outcome	Reduced model predictors	ΔAIC	ΔBIC
Pelvis_Angle (deg)	SeatbackAngle + Headrest_bin + Gender_bin	-1.9	-11.8
T12_X (mm)	SeatbackAngle + Headrest_bin	-2.29	-15.5
T12_Z (mm)	SeatbackAngle + Headrest_bin	-6.09	-19.3
C7_X (mm)	SeatbackAngle + Headrest_bin + Age + BMI + ESH	-1.99	-5.29
C7_Z (mm)	SeatbackAngle + Headrest_bin + BMI + ESH	-2.55	-9.15
C0_X (mm)	SeatbackAngle + Headrest_bin + Age + BMI + ESH	-1.99	-5.29
C0_Z (mm)	SeatbackAngle + Headrest_bin + ESH	-2.66	-12.6

Appendix A.8: Model-specific residual distances in the pelvis-angle comparison

This appendix provides HBM-specific information of the cross-HBMs pelvis-alignment comparison reported in Table 1. For each pelvis-angle definition, the ASIS and pubic symphysis coordinates of the five HBMs were compared with the corresponding five-model landmark centroid calculated in the sagittal plane. The Euclidean distance of each model from the ASIS centroid and from the pubic symphysis centroid was calculated separately. A combined ASIS + pubic symphysis distance was then calculated for each model as

$$D_m = \sqrt{\frac{d_{\text{ASIS},m}^2 + d_{\text{pubic},m}^2}{2}},$$

where $d_{\text{ASIS},m}$ and $d_{\text{pubic},m}$ are the distances of model m from the ASIS and pubic symphysis centroids, respectively. Lower values indicate closer agreement with the five-model landmark centroid after the corresponding pelvis-angle normalisation according to the definition.

Table A.4 HBM-specific D_m distance from the five-HBM centroid and for each pelvis-angle definition. All values are reported in millimetres.

Pelvis-angle definition	GHBMC	HANS	THUMS	ViVA+	SAFER
HJC translation only	12.16	1.86	14.33	8.10	5.62
HJAS	6.05	2.17	12.40	4.02	4.23
HJLS	8.73	6.11	19.38	3.45	4.78
SS	12.60	3.28	13.43	5.79	5.82
NPA	9.01	1.83	20.71	6.01	5.91
ASLS	8.45	6.38	22.19	4.32	5.94